Large eddy simulations of high Reynolds number turbulence based on interscale energy transfer among resolved scales

J. Andrzej Domaradzki*

Department of Aerospace and Mechanical Engineering, University of Southern California, Los Angeles, California 90089-1191, USA

(Received 18 December 2020; accepted 6 April 2021; published 20 April 2021)

In the present work we show how the subgrid-scale (SGS) energy transfer among resolved scales in large eddy simulations (LESs) can be used to evaluate unknown constants in SGS models and derive new models. The essence of the method is that for a given LES velocity field energy transfers among resolved scales can be computed without reference to a particular SGS model and then used to estimate the total SGS energy transfer for an unknown, full velocity field. The total transfer becomes a physical constraint on any proposed SGS model and can be used to obtain and update model constants at each time step in actual LES, allowing self-contained simulations. The method is evaluated by implementing it in LESs of high Reynolds number isotropic turbulence and for several classical SGS modeling expressions. It is shown that the performance of models depends not only on their ability to capture the total SGS dissipation (which is enforced by the method) but also by distribution of the SGS dissipation among scales of motion (which is enforced by a model). However, the main conclusion is that a broad class of modeling expressions that only qualitatively approximate the SGS dissipation distribution among scales perform very well in LESs as long us the total dissipation constraint is satisfied. We also discuss the relation of the method to the well-known dynamic modeling procedure.

DOI: 10.1103/PhysRevFluids.6.044609

I. INTRODUCTION

The equations for large eddy simulations (LESs) are traditionally obtained with the filtering approach proposed by Leonard [1] where a spatial filter that strongly attenuates scales of motion smaller than the prescribed filter width Δ is applied to the Navier-Stokes equations. Alternatively, when Fourier spectral methods are used it is natural to use a sharp spectral filter which offers two benefits: a clear distinction between resolved and unresolved scales delineated by a wave number cutoff k_c, and a clean interpretation of physical quantities in the framework of classical phenomenology and analytical theories of turbulence which are formulated in terms of Fourier modes.

If the filtered quantities are denoted by an overbar, the LES equations for an incompressible flow become

$$\frac{\partial}{\partial t}\overline{u}_i + \frac{\partial}{\partial x_j}\overline{u}_i\,\overline{u}_j = -\frac{1}{\rho}\frac{\partial}{\partial x_i}\overline{p} + \nu\frac{\partial^2}{\partial x_j \partial x_j}\overline{u}_i - \frac{\partial}{\partial x_j}\tau_{ij}, \tag{1}$$

$$\frac{\partial}{\partial x_i}\overline{u}_i = 0, \tag{2}$$

*jad@usc.edu

where $u_i = (u_1, u_2, u_3) = (u, v, w)$, p, and ν are the velocity, pressure, and kinematic viscosity, respectively, and τ_{ij} is the subgrid-scale (SGS) stress tensor

$$\tau_{ij} = \overline{u_i u}_j - \overline{u}_i \, \overline{u}_j. \tag{3}$$

The form of Eqs. (1) and (2) requires that the filtering and differentiation commute ([2,3]). In practice, however, the above equations are frequently the starting point in SGS modeling without regard to formal requirements for their derivation in the filtering framework. The important point is that the LES equations have the form of the Navier-Stokes equations for the filtered velocity $\overline{u}_i$ plus the additional force term which is the divergence of the subgrid scale stress tensor (3), and which is required to close the LES equations. Various SGS models differ in how the SGS stress tensor is expressed (or modeled) in terms of the filtered velocity $\overline{u}_i$.

There are a number of excellent reviews of theory and practice of SGS modeling (e.g., [4–9]), but they will be discussed in detail only when needed for the purposes of this work. However, it is useful to note that despite a significant effort in this field over more than 50 years, two broad categories of successful models (as indicated by their widespread use in practice) date to the period between the early 1960s and early 1990s. Among the most important category are the eddy viscosity models. Their origin goes back to Boussinesq who proposed that the effects of turbulence can be accounted for by the viscosity increased over its value in laminar flows. With the advent of computers and attempts to perform general circulation simulations, the eddy viscosity concept was used by Smagorinsky [10] to model "The lateral transfer of momentum and heat by the nonlinear diffusion, which parametrically is supposed to simulate the action of motions of sub-grid scale. . . ," starting the modern era of LES and SGS modeling. Later the Smagorinsky model coupled with the dynamic procedure of Germano [11] has become probably most widely used tool in LESs of a variety of turbulent flows. Another approach to LESs, known as implicit large eddy simulations (ILESs), was originally proposed by Boris *et al.* [12]. It is based on the observation that truncation errors in certain discretizations of Navier-Stokes equations introduce numerical dissipation with the implicit effects of the discretization qualitatively similar to the effects of the explicit SGS models. Such similarities are used to support the ILES approach as a turbulence modeling tool [13–15]. Those, as well as other SGS modeling procedures, are normally evaluated by performing multiple LESs for different physical conditions and adjusting model constants iteratively until the best agreement with appropriate benchmarks is reached. A typical example is a need to modify a theoretically predicted value of the constant for the classical Smagorinsky model depending on type of flow ($C_S = 0.18$ for homogenous turbulence, derived by Lilly [16]; $C_S = 0.21$ for Rayleigh-Bénard convection used by Eidson [17], and Table 1 in that reference also lists nine values of C_S ranging from 0.10 to 0.24 for different turbulent flows; $C_S = 0.06$–0.1, depending on Reynolds number, inferred from the dynamic model LESs for channel flow by Piomelli [18]). In order to avoid ambiguities in comparing LES results with direct numerical simulation (DNS) benchmarks Toosi and Larsson [19] developed a method to evaluate quantitatively the relative error in such comparisons.

The category of SGS models of interest in this paper was originated by Kraichnan [20] who was first to employ an analytical theory of turbulence, the test field model (TFM), to compute a scale-dependent eddy viscosity. It should be stressed that even though the term "eddy viscosity" is used, the primary quantity in the model is the energy transfer across a wave number cutoff k_c between large scales ($k < k_c$) and subgrid scales ($k > k_c$), i.e., the SGS energy transfer which is then appropriately normalized to cast it in a form of a more familiar concept of the eddy viscosity. Results of Kraichnan's analysis were confirmed later by Leslie and Quarini [21] who also extended the methodology to investigate the energy backscatter and effects of graded filters on the eddy viscosity expressions. Chollet and Lesieur [22] provided an additional verification in the framework of eddy damped quasi-normal Markovian (EDQNM) approximation. A good overview of these approaches can be found in Lesieur [23] and Lesieur *et al.* [24]. The theoretical eddy viscosity obtained in these publications is immediately applicable to the spectral energy equation and in the same form to LESs of isotropic turbulence performed using Fourier spectral methods (see [5]). However, there are several limitations of this approach. The derivation assumes an infinite inertial

range spectrum and model constants depend on a value of the Kolmogoroff constant. It is also not obvious how to extend the model to inhomogeneous turbulence which requires the physical space representation. One possible approach is the structure-function model proposed by Métais and Lesieur [25]. Despite these uncertainties, the fundamental strength of this model is that it is based on a physically sound theory, offering a major advantage over many typical models based on phenomenological considerations.

In this paper we approach the SGS modeling task along similar lines, i.e., employing a computed SGS energy transfer. The main difference is that the SGS transfer is obtained not from the theory but directly from evolving LES fields. The methodology is informed by an extensive literature on the subject of interscale energy transfer in turbulence obtained through analyses of DNSs. The methodology used for the analysis of interscale energy transfer is outlined by Domaradzki and Rogallo [26], Domaradzki *et al.* [27], and Domaradzki and Liu [28]. Studies based on this methodology for isotropic turbulence were conducted by Domaradzki [29], Domaradzki and Rogallo [26], Yeung and Brasseur [30], and Domaradzki *et al.* [31–33]. Using the same framework studies of the energy exchange between scales of turbulence in low Reynolds number shear flows have been carried out by Domaradzki *et al.* [27]. More recently extensive investigations of energetics for turbulent channel flow at high Reynolds numbers have been carried out by Lee and Moser [34] and Cimarelli *et al.* [35,36]. The proposed approach offers a synthesis of information available from that research for the task of SGS modeling. The first attempt to derive a SGS model within this framework was made by Anderson and Domaradzki [37]. The model's implementation in LESs of channel flow showed good performance for Reynolds numbers up to $\mathrm{Re}_\tau = 2000$. However, the implementation was not able to provide sufficient levels of SGS dissipation in LESs of isotropic turbulence in the limit of very high Reynolds numbers [38]. In the present work the failure of the original implementation is traced back to the scale distribution of the modeled SGS dissipation, and a modified approach is developed that leads to excellent results in LESs of isotropic turbulence in the invicid limit. The essence of the method is that for a given LES velocity field energy transfers among resolved scales can be used to estimate the total SGS energy transfer for an unknown, full velocity field. The total transfer then becomes a physical constraint on any modeled scale distribution of the transfer and is used to obtain and update model constants at each time step in actual LESs, leading to self-contained simulations.

II. SELECTION OF FLOW AND NUMERICAL METHODS

For the purposes of developing and testing the proposed modeling procedure we choose isotropic, homogeneous turbulence at very high Reynolds numbers, simulated using pseudospectral Fourier methods. This choice could be criticized as of limited interest to the current LES practice preoccupied with wall bounded flows in complex geometries, wall modeling for high Reynolds/Mach number incompressible/compressible flows, and additional physical phenomena such as heat transfer, chemical reactions, etc. Nevertheless we believe that our choice is an unavoidable first step, on several counts, to advance the proposed method. First, isotropic turbulence is the case for which physical theories and DNSs provide most complete and unambiguous information about details of energy transfer among scales of motion. Therefore, isotropic turbulence is the case for which that information can be most directly exploited in model development. Second, sometimes SGS models that show promise in LESs of low Reynolds number turbulence may fail catastrophically at high Reynolds numbers. This is due to the fact that as the viscous dissipation in LESs diminishes with an increasing Reynolds number, the model alone may fail to provide sufficient SGS dissipation. The best example of such a behavior is the similarity model of Bardina *et al.* [39] (see Fig. 2 below). Third, pseudospectral Fourier methods largely eliminate the effects of numerical dissipation in simulations. This is important because unquantified numerical dissipation in simulations performed with finite volume/finite differences methods often clouds interpretation of LES results, even to the extend of suggesting that a SGS model is entirely unnecessary (ILESs). Obviously, no such a conclusion will be reached in pseudospectral simulations in the inviscid limit where an explicit

source of dissipation, e.g., a SGS model, is required to prevent a tendency toward an equipartition of energy for a finite number of wave number modes.

For the purpose of simulations the flow is assumed to be contained in a cube of side $L = 2\pi$, and periodic boundary conditions in all three spatial directions are imposed on the independent variables. The domain is discretized in physical space using N uniformly spaced grid points in each direction resulting in a mesh size $\Delta x = L/N$ and a total of N^3 grid points. The independent variables are transformed between physical and spectral space using the discrete Fourier transform

$$\mathbf{u}(\mathbf{k}) = \frac{1}{N^3} \sum_{\mathbf{x}} \mathbf{u}(\mathbf{x}) \exp(-i\mathbf{k} \cdot \mathbf{x}) \tag{4}$$

and the inverse transform

$$\mathbf{u}(\mathbf{x}) = \sum_{\mathbf{k}} \mathbf{u}(\mathbf{k}) \exp(i\mathbf{k} \cdot \mathbf{x}), \tag{5}$$

where $\mathbf{x}$ are the mesh points in physical space and $\mathbf{k}$ are the discrete wave numbers with components $k_i = \pm n_i \Delta k,\ n_i = 0,\ 1,\ 2,\ \ldots,\ N/2,\ i = 1,\ 2,\ 3,$ and $\Delta k = 2\pi/L = 1$. The distinction between physical and spectral representation for a given quantity is made through its argument $\mathbf{x}$ or $\mathbf{k}$, respectively.

For homogeneous turbulence, Navier-Stokes equations [Eqs. (1)–(2) with the SGS term neglected] can be transformed into spectral (Fourier) space (see, e.g., Lesieur [23] and Pope [8]):

$$ik_n u_n(\mathbf{k}, t) = 0, \tag{6}$$

$$\left(\frac{\partial}{\partial t} + \nu k^2\right) u_n(\mathbf{k}, t) = N_n(\mathbf{k}, t) - ik_n p(\mathbf{k}, t), \tag{7}$$

where wave numbers $\mathbf{k}$ are associated with scales of turbulent motions and N_n is the Fourier transform of the nonlinear term

$$N_n(\mathbf{k}, t) = -ik_j \int d\mathbf{p}\ u_j(\mathbf{p}, t) u_n(\mathbf{k} - \mathbf{p}, t). \tag{8}$$

The equation for the energy amplitudes $\frac{1}{2}|u(\mathbf{k}, t)|^2 = \frac{1}{2} u_n(\mathbf{k}, t) u_n^*(\mathbf{k}, t)$, where the asterisk denotes a complex conjugate, follows from (7)

$$\frac{\partial}{\partial t} \frac{1}{2} |u(\mathbf{k}, t)|^2 = -2\nu k^2 \frac{1}{2} |u(\mathbf{k}, t)|^2 + T(\mathbf{k}, t), \tag{9}$$

where $T(\mathbf{k}, t)$ is the nonlinear energy transfer

$$T(\mathbf{k}, t) = \mathrm{Re}[u_n^*(\mathbf{k}) N_n(\mathbf{k}, t)], \tag{10}$$

and Re is the real part of a complex expression. Physical quantities of interest for isotropic turbulence are described in terms of the scalar wave number $k = |\mathbf{k}|$ by averaging over thin spherical shells defined for an arbitrary quantity $f(\mathbf{k})$ as

$$\langle f(\mathbf{k}) \rangle = \frac{1}{N_{\mathbf{k}}} \sum_{\mathbf{k}} f(\mathbf{k}), \tag{11}$$

where $\langle \ldots \rangle$ denotes the shell average and the summation extends over all $N_{\mathbf{k}}$ modes in the shell of thickness Δk centered at $k = |\mathbf{k}|$. For instance, the energy spectrum is defined as

$$E(k, t) = 4\pi k^2 \langle \tfrac{1}{2} u_n(\mathbf{k}, t) u_n^*(\mathbf{k}, t) \rangle \tag{12}$$

and the corresponding dissipation spectrum is

$$D(k, t) = 2\nu k^2 E(k, t). \tag{13}$$

Similarly, $T(\mathbf{k}, t)$ integrated in spectral space over spheres of radius $k = |\mathbf{k}|$, provides the classical energy transfer $T(k, t)$ in the spectral energy equation

$$\frac{\partial}{\partial t}E(k,t) = -2\nu k^2 E(k,t) + T(k,t). \tag{14}$$

For brevity, in subsequent formulas, explicit time dependence will be omitted.

The equations are solved using a pseudospectral numerical method of Rogallo [40] in the implementation of Yeung and Pope [41]. We have employed the forcing scheme of Sullivan *et al.* [42] in which the total energy of several low wave number modes is kept constant while evolution of individual modes through nonlinear interactions, subject to the global energy constraint, is allowed. Specifically, the sum of squared amplitudes of velocity modes in a sphere of radius $K_f = 3.5\Delta k$ is kept constant. This is accomplished by multiplying all modes in the forced sphere by the same constant factor, usually not larger than 1.002, at the end of each time step. This restores the energy in the sphere to the value at the beginning of the time step.

Turbulence is characterized by several physical parameters that are related to spectral quantities. The integral of $E(k)$ over k gives turbulent kinetic energy per unit mass $\frac{3}{2}u'^2$, where u' is the r.m.s. turbulent velocity. The integrated dissipation spectrum gives the dissipation rate of the turbulent kinetic energy, ε. The Taylor microscale is computed as $\lambda = (15u'^2\nu/\varepsilon)^{1/2}$, and the microscale Reynolds number is $\mathrm{Re}_\lambda = u'\lambda/\nu$. An important timescale for the evolution of turbulence is the large eddy turnover time $T_e = L_p/u'$, where L_p is the integral length scale

$$L_p = \frac{\pi}{2u'^2}\int_0^\infty k^{-1}E(k)\,dk. \tag{15}$$

The macroscale Reynolds number is defined using L_p as $\mathrm{Re} = u'L_p/\nu$.

III. SGS QUANTITIES AND MODELING EXPRESSIONS

In spectral LESs, a cutoff wave number k_c is introduced to separate resolved and subgrid scales (SGSs), and evolution equations for the resolved scales $k \leqslant k_c$ are sought. The spectral energy equation for scales $k \leqslant k_c$ is

$$\frac{\partial}{\partial t}E^<(k|k_c) = T^<(k|k_c) + T_{\mathrm{SGS}}(k|k_c) - 2\nu k^2 E^<(k|k_c), \tag{16}$$

where the notation $Q^<(k|k_c)$ indicates that, in computing the quantity Q, only modes satisfying the inequality $k \leqslant k_c$, i.e. scales that are fully known in LESs with the cutoff k_c, are retained. The SGS energy transfer term, $T_{\mathrm{SGS}}(k|k_c)$, is the only term in (16) that requires information about modes $k > k_c$, which are unknown in LESs. Since Eq. (16) is simply Eq. (14), rewritten for modes $k \leqslant k_c$, the SGS energy transfer term is

$$T_{\mathrm{SGS}}(k|k_c) = T(k) - T^<(k|k_c), \;\; k \leqslant k_c, \tag{17}$$

where $T(k)$ is the full nonlinear transfer from Eq. (14) in the resolved range $k \leqslant k_c$. Equation (17) provides a simple method to compute $T_{\mathrm{SGS}}(k|k_c)$ through two calculations of the transfer term and was first used by Domaradzki *et al.* [29,43] in the context of the analysis of DNS data. Note that for $T^<(k|k_c)$ the operation signified by superscript "<" is not simply a sharp spectral filter applied to $T(k)$. The filter is applied to the velocity field $u_n(\mathbf{k})$ and then the regular transfer term expression (10) is used for the filtered field to produce $T^<(k|k_c)$. Therefore, $T^<(k|k_c)$ is effectively the energy transfer for a subset of modes in the computational domain.

Energy dynamics in theories of turbulence are often described by an equation for the energy of all modes below k_c, $\mathcal{E}(k_c) \equiv \int_0^{k_c} E(k)\,dk$,

$$\frac{\partial}{\partial t}\mathcal{E}(k_c) = -2\nu\int_0^{k_c} k^2 E(k)\,dk + \Pi(k_c), \tag{18}$$

where the classical energy flux

$$\Pi(k_c) = \int_0^{k_c} T(k)\, dk \tag{19}$$

provides the energy transfer rate from all scales below k_c to those above k_c. Because the nonlinear term in Navier-Stokes equations is energy conserving the transfer $T(k)$ integrated over entire wave number domain $[0, k_{\max} = N/2]$ vanishes and $\Pi(k_{\max}) = 0$, i.e., there is no energy flux to scales that are not represented in the domain. For the same reason the transfer term $T^<(k|k_c)$ for a subset of modes obtained using sharp spectral filter with cutoff k_c is energy conserving, i.e., $\int_0^{k_c} T^<(k|k_c)\, dk = 0$. Note that integrating equation (16) over resolved wave numbers gives Eq. (18) for $\mathcal{E}(k_c)$. Because the term $\int_0^{k_c} T^<(k|k_c)\, dk$ vanishes, the SGS energy transfer integrated over its wave number domain, the so-called total SGS dissipation, satisfies the condition

$$\epsilon_{\rm SGS}(k_c) \equiv \int_0^{k_c} T_{\rm SGS}(k|k_c)\, dk = \Pi(k_c). \tag{20}$$

The total SGS dissipation can also be computed using standard LES formulas in the physical space representation

$$\epsilon_{\rm SGS}(\mathbf{x}) = \tau_{ij}(\mathbf{x})\overline{S}_{ij}(\mathbf{x}), \tag{21}$$

where the SGS stress tensor is given by (3) and $\overline{S}_{ij}$ is the resolved rate-of-strain tensor

$$\overline{S}_{ij} = \frac{1}{2}\left(\frac{\partial \overline{u}_i}{\partial x_j} + \frac{\partial \overline{u}_j}{\partial x_i}\right). \tag{22}$$

In the above formulas the overbar denotes a general filtering procedure, and the space dependent SGS dissipation represents the energy transfer term in LES equations. For a spherical, sharp spectral filter with cutoff k_c in the above formulas the filtering and differentiation are performed in spectral space and multiplication of τ_{ij} and $\overline{S}_{ij}$ in the physical space. The total SGS dissipation is

$$\epsilon_{\rm SGS}(k_c) = \frac{1}{N^3}\sum_{\mathbf{x}} \epsilon_{\rm SGS}(\mathbf{x}), \tag{23}$$

with summation over all N^3 mesh points $\mathbf{x}$. Note, however, that while values of integrated SGS transfers (20) and (23) are the same, there is no equivalent spectral space formula corresponding to the local SGS dissipation in the physical space representation (21).

Note that negative values of $T(k)$ signify energy losses at wave numbers k. However, traditionally, the energy flux Π, the SGS energy transfer $T_{\rm SGS}$, and the SGS dissipation $\epsilon_{\rm SGS}$ are chosen to be positive if the resolved scales experience energy loss. For consistency with $T(k)$, we are not adopting this latter convention. If definitions (17)–(21) are employed, negative $\Pi(k_c)$ will signify energy losses for the range $k \leqslant k_c$ and negative values of $T_{\rm SGS}(k|k_c)$ will represent energy losses at k through the SGS interactions. Similarly, the SGS dissipation $\epsilon_{\rm SGS}(k_c)$ in Eq. (23) will be negative. When positive values of these quantities are needed we will simply use absolute values.

The SGS spectral energy equation can be formally rewritten as

$$\frac{\partial}{\partial t}E^<(k|k_c) = T^<(k|k_c) - 2\nu_{th}(k|k_c)k^2E^<(k|k_c) - 2\nu k^2E^<(k|k_c), \tag{24}$$

where the SGS energy transfer is expressed in the same functional form as the molecular dissipation term by introducing the theoretical eddy viscosity

$$\nu_{th}(k|k_c) = -\frac{T_{\rm SGS}(k|k_c)}{2k^2E^<(k|k_c)}. \tag{25}$$

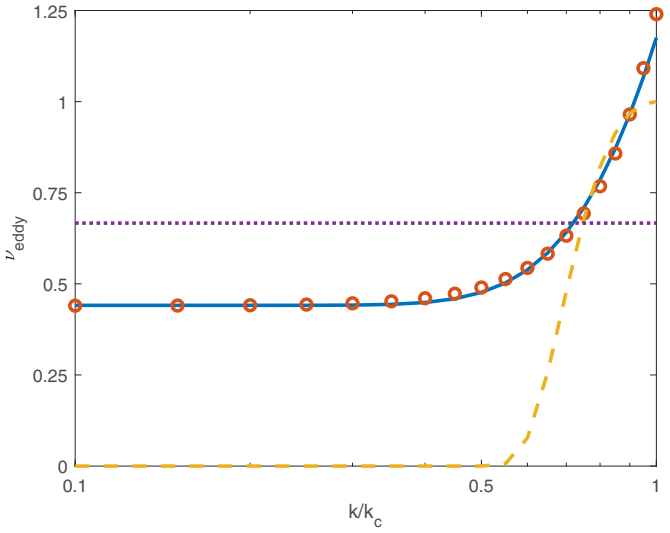

FIG. 1. Spectral eddy viscosity functions. Solid line: Chollet-Lesieur, Eq. (27); symbols ○: function $C_2 f_2$, Eq. (29); dotted line: constant eddy viscosity, Eq. (28); broken line: SVV viscosity, Eq. (30).

Frequently it is nondimensionalized using values of the energy spectrum at the cutoff

$$\nu_{th}^{+}(k|k_c) = \frac{\nu_{th}(k|k_c)}{\sqrt{E(k_c)/k_c}}. \tag{26}$$

Assuming infinite inertial range spectrum $k^{-5/3}$, theoretical formulas for $T_{\mathrm{SGS}}(k|k_c)$ can be computed numerically [20,22,23], and the normalized eddy viscosity (26) is well fitted by the expression given by Chollet [44]

$$\nu_{th}^{+}(k|k_c) = {C_K}^{-3/2}\left(0.441 + 15.2e^{-3.03k_c/k}\right) \equiv {C_K}^{-3/2} f_1(k|k_c), \tag{27}$$

where C_K is the Kolmogorov constant, taken usually as 1.4, and f_1 is a spectral model shape function.

In order to allow implementation of the spectral eddy viscosity also for LESs in the physical space variables two approaches are possible. The simplest is to use a constant spectral eddy viscosity that provides the same value of the total SGS energy transfer as the k-dependent eddy viscosity (27). For the assumed $k^{-5/3}$ energy spectrum such a constant spectral eddy viscosity from [25] is

$$\nu_{\mathrm{const}}^{+}(k|k_c) = \frac{2}{3}{C_K}^{-3/2} f_0(k|k_c), \tag{28}$$

where the shape function $f_0 = 1$. The second approach is to replace function $f_1(k|k_c)$ in (27) by a different function that can be easily interpreted in the physical space. We propose the following expression:

$$f_1(k|k_c) \approx C_2(D_2 + (k/k_c)^4) \equiv C_2 f_2(k|k_c), \quad \text{where } C_2 = 0.8 \text{ and } D_2 = 0.55, \tag{29}$$

which is similar to a physical space eddy viscosity fit proposed by Lesieur *et al.* [24,25] in the context of the structure function SGS model. For LES equations in the physical space the constant spectral eddy viscosity (28) will lead to a standard Laplacian term ∇^2 and the approximation (29) to a sum of the Laplacian and a hyperviscosity term proportional to ∇^6. Additionally, adjusting constant D_2 in (29) allows us to control relative contributions to the SGS transfer from the eddy viscosity plateau and its cusp (see Fig. 1).

Another class of spectral models, qualitatively different from the models outlined above, are spectral vanishing viscosity (SVV) models introduced by Karamanos and Karniadakis [45]. The functional form of the kernel of a SVV model proposed by Lamballais *et al.* [46] is

$$f_3(k|k_c) = \nu^+_{SVV}(k|k_c) = \begin{cases} 0 & \text{if } k \leqslant Ak_c, \\ \exp\left[-\left(\frac{1-k/k_c}{A-k/k_c}\right)^2\right] & \text{otherwise.} \end{cases} \tag{30}$$

The main difference between the SVV viscosity and the previous models is that a fraction of the resolved wave number range, defined by constant A, is unaffected by the model. We will choose here $A = 0.35$ to confine the action of the eddy viscosity to one half of the wave number range adjacent to the cutoff k_c. In Fig. 1 we plot spectral shapes of all four eddy viscosity models. It should be added that the general concept of the wave-number-dependent eddy viscosity for homogenous turbulence is strongly supported by an independent analysis of Langford and Moser [47], who found that it was the dominant term in a multiterm formulation of the optimal SGS model. Thus while there might be differences between specific eddy viscosity formulas, there is a general agreement that the formulas considered in this paper constitute a proper framework for LES modeling of homogenous, isotropic turbulence. Note also that we are not attempting to normalize the curves in Fig. 1 (e.g., by the maximum value) because in the method proposed in the next section each spectral function will be multiplied by an appropriate constant that will force the model SGS dissipation to be equal to the SGS dissipation determined for a given velocity field independently of the model. It will be shown that enforcing this condition allows for a greater freedom in choosing the form of eddy viscosity models.

IV. DETERMINATION OF THE TOTAL SGS ENERGY TRANSFER FROM RESOLVED LES FIELDS

A. Interscale energy transfer

For the purposes of model development we follow Domaradzki *et al.* [28,33] and Anderson and Domaradzki [37] and decompose the wave number space into three discrete wave number regions denoted by R_1, R_2, R_3:

$$\begin{aligned} R_1&: \quad 0 \leqslant k < k_1, \\ R_2&: \quad k_1 \leqslant k < k_2, \\ R_3&: \quad k_2 \leqslant k < \infty, \end{aligned} \tag{31}$$

where $k_2 = k_c$ is the SGS wave number cutoff and $k_1 = ak_c$ is an intermediate cutoff in the resolved range (constant $a < 1$, usually set to $1/2$). Thus region R_3 represents SGS scales, unresolved in LESs, and regions R_1 and R_2 represent respective large and small resolved scales. Using this decomposition the nonlinear term (8) can be decomposed as

$$N_n(\mathbf{k}) = \sum_{p=1}^{3}\sum_{q\geqslant p}^{3}\sum_{m=1}^{3} N_n^{pqm}(\mathbf{k}). \tag{32}$$

Each term in (32) describes effects of nonlinear interactions between two regions p and q on the third region m. The corresponding energy transfer term is

$$T^{pqm}(\mathbf{k}) = \mathrm{Re}[u_n^*(\mathbf{k})N_n^{pqm}(\mathbf{k})], \tag{33}$$

which describes the energy rate change for modes in region m caused by nonlinear interactions between regions p and q. The decomposition of the energy transfer term (10) is

$$T(\mathbf{k}) = \sum_{p=1}^{3}\sum_{q\geqslant p}^{3}\sum_{m=1}^{3} T^{pqm}(\mathbf{k}). \tag{34}$$

Several familiar expressions in SGS modeling can be rewritten in this notation. The SGS transfer for the cutoff k_c is

$$T_{\mathrm{SGS}}(\mathbf{k}|k_c) = T^{131} + T^{231} + T^{331} + T^{132} + T^{232} + T^{332}, \tag{35}$$

where terms on the r.h.s. account for interactions between two bands (first two indices) that must involve SGS band 3, affecting resolved bands (third index: bands 1 and 2). The SGS transfer for the cutoff $k_1 = ak_c$ is

$$T_{\mathrm{SGS}}(\mathbf{k}|ak_c) = T^{121} + T^{131} + T^{221} + T^{231} + T^{331}, \tag{36}$$

where terms on the r.h.s. account for interactions between two bands (first two indices) that must involve SGS bands 2 and/or 3, affecting resolved band 1 (third index). Truncating (35) to region 1 gives

$$[T_{\mathrm{SGS}}(\mathbf{k}|k_c)]^1 = T^{131} + T^{231} + T^{331}, \tag{37}$$

and combining this expression with (36) provides the Germano identity

$$T_{\mathrm{SGS}}(\mathbf{k}|ak_c) - [T_{\mathrm{SGS}}(\mathbf{k}|k_c)]^1 = T^{121} + T^{221}, \tag{38}$$

where the r.h.s. is the SGS transfer within resolved range $R_1 \cup R_2$ with cutoff k_1, i.e., with terms on the r.h.s. accounting for interactions involving bands 1 and 2, affecting band 1 (third index)

$$T^{\mathrm{res}}_{\mathrm{SGS}}(\mathbf{k}|ak_c) = T^{121} + T^{221}. \tag{39}$$

Note that in symbolic equations above terms with all three same indices such as T^{111} are neglected because, as discussed before, nonlinear interactions among any subset of modes obtained using sharp spectral filters are energy conserving and do not affect total energy of any band.

The original interscale transfer model (ITM) of Anderson and Domaradzki [37] is based on the decomposition of the energy transfer within the resolved range scales

$$T^{\mathrm{res}}(\mathbf{k}|k_c) = T^{111} + T^{121} + T^{221} + T^{112} + T^{122} + T^{222}. \tag{40}$$

In this decomposition terms T^{111} and T^{222} are energy conserving, and T^{112} and T^{122} will lead to energy accumulation in range R_2 unless SGS interactions with scales in R_3 keep removing the energy from R_2. The ITM model attempts to model this SGS energy transfer by explicit cancellation of the energy accumulation terms in (40)

$$T^{\mathrm{res}}_{\mathrm{LES}}(\mathbf{k}|k_c) = T^{\mathrm{res}}(\mathbf{k}|k_c) - T^{112} - T^{122}, \tag{41}$$

where the SGS dissipation of the ITM model is

$$T^{\mathrm{ITM}}_{\mathrm{SGS}}(\mathbf{k}|k_c) = -T^{112} - T^{122}. \tag{42}$$

The difficulties met by this version of the model at high Reynolds numbers, noted in the Introduction, can be traced to distribution of SGS energy transfer in wave number space. Because the energy transfer between two neighboring wave number bands is most effective in the vicinity of the band boundary, the model expression (42) overestimates the SGS dissipation at $k = k_1 = ak_c$ and underestimates it in the vicinity of the actual LES cutoff k_c. This leads to failure at high Reynolds numbers when effects of the molecular viscosity are not available to counteract this behavior, a situation very similar to the origin of failure of a pure similarity model at high Reynolds numbers. Because of that the model (42) has been abandoned. However, the above observations suggested a modified approach, discussed in this paper, that removes the source of difficulties by rescaling the energy transfer from the test cutoff k_1 to the actual LES cutoff k_c.

Since $T^{\mathrm{res}}_{\mathrm{SGS}}$ can be computed directly for a given LES field we investigate if that fact can be used to estimate the SGS energy transfer for the full velocity fields with cutoff k_c. To be more specific we

assume that the velocity field is consistent with the infinite inertial range spectrum $k^{-5/3}$, $k_1 = \frac{1}{2}k_c$, and we focus on the total transfers, integrated over respective wave number domains:

$$T_{\rm SGS}(k_c) = \int_0^{k_c} d\mathbf{k} T_{\rm SGS}(\mathbf{k}|k_c) = \varepsilon_{\rm SGS}(k_c), \tag{43}$$

$$T^{\rm res}_{\rm SGS}\left(\frac{1}{2}k_c\right) = \int_0^{\frac{1}{2}k_c} d\mathbf{k} T^{\rm res}_{\rm SGS}\left(\mathbf{k}|\frac{1}{2}k_c\right). \tag{44}$$

Note that integrated SGS transfer terms are indicated by dependence only on the cutoff wave number but not on $\mathbf{k}$. In this notation the Germano identity (38) integrated over region R_1 becomes

$$T_{\rm SGS}\left(\frac{1}{2}k_c\right) - \int_0^{\frac{1}{2}k_c} d\mathbf{k} T_{\rm SGS}(\mathbf{k}|k_c) = T^{\rm res}_{\rm SGS}\left(\frac{1}{2}k_c\right). \tag{45}$$

For the infinite inertial range energy flux across the spectrum is constant, allowing us to replace the first term in (45) by $T_{\rm SGS}(k_c)$. The second term is a fraction of the total transfer $T_{\rm SGS}(k_c)$ because the integration interval covers only a fraction of a wave number domain contributing to $T_{\rm SGS}(k_c)$, formally

$$\int_0^{\frac{1}{2}k_c} d\mathbf{k} T_{\rm SGS}(\mathbf{k}|k_c) = bT_{\rm SGS}(k_c), \tag{46}$$

where b is a constant to be determined. With the above substitutions the equation for $T_{\rm SGS}(k_c)$ becomes

$$T_{\rm SGS}(k_c) = \frac{1}{1-b} T^{\rm res}_{\rm SGS}\left(\frac{1}{2}k_c\right). \tag{47}$$

The constant b can be obtained using several approaches. One is by using properties of the infrared scale locality functions for the energy flux $\Pi(k|k_c)$ introduced by Kraichnan [48,49]. $\Pi(k|k_c)$ measures the amount of the energy flux through k_c that is due to nonlinear interactions involving wave numbers less than k. The classical scaling is $(k/k_c)^{4/3}$, implying that contribution of scales $k < \frac{1}{2}k_c$ to the energy transfer across k_c is the fraction $b = 2^{-4/3} = 0.40$ of the total transfer at k_c. We have also reanalyzed DNS data from isotropic simulations performed with 512^3 resolution in our previous work [33,50], obtaining for the inertial range part of the spectrum value $b = 0.33$–0.34. Assuming applicability of the spectral eddy viscosity form (29), the constant b can also be obtained as

$$b = \frac{\int_0^{\frac{1}{2}k_c} f_2(k|k_c) 2k^2 E(k)\, dk}{\int_0^{k_c} f_2(k|k_c) 2k^2 E(k)\, dk} \approx 0.36. \tag{48}$$

Finally, assuming a constant eddy viscosity in the formula above, i.e., $f_2 = f_0 = 1$ will give the same result as the scaling theory, $b = 0.4$. These results are largely consistent with each other, and there are no strong reasons to prefer any particular choice. We have selected $b = 0.40$ for the purposes of this work. For this choice the total SGS transfer is expressed in terms of the resolved SGS transfer with a fortuitous prefactor

$$T_{\rm SGS}(k_c) = \frac{5}{3} T^{\rm res}_{\rm SGS}(\frac{1}{2}k_c). \tag{49}$$

It is well known that a SGS model must provide sufficient total SGS dissipation to be successful. For a given LES velocity field the above expression provides the total SGS dissipation computed from physics of interscale interactions for that field. Because of that link to physics of energy transfer we expect that (49) can serve as an useful constraint on SGS models. A related approach was considered by Park and Mahesh [51], who used a SGS dissipation of the dynamic Smagorinsky model for a given velocity field as a constraint for another, improved SGS model. Here we rely on

the physical prediction of the total SGS dissipation (47), which will become a first-order condition that must be satisfied by any successful SGS model for that field. However, as we will see, the total SGS dissipation must be distributed appropriately among all scales $k < k_c$ to obtain good LES results. The distribution of the total SGS dissipation is a higher order condition since many different distributions will produce very similar LES results. We will consider SGS dissipation distributions given by shape functions for several spectral eddy viscosity models discussed before (27)–(30). Specifically, the eddy viscosity implemented in actual LESs is

$$\nu_{\text{eddy}}(k|k_c) = C_m(t) f_i(k|k_c), \quad i = 0, 1, 2, 3, \tag{50}$$

where functions f_i are given in (27)–(30). The multiplicative constant $C_m(t)$ is determined from the first-order constraint

$$C_m(t) = \frac{T_{\text{SGS}}(k_c)}{\int_0^{k_c} f_i(k|k_c) 2k^2 E(k)\, dk}. \tag{51}$$

In (51) $T_{\text{SGS}}(k_c)$ is expressed in terms of SGS transfer among resolved scales (49), computed at each time step in LESs with the spectral eddy viscosity given by (50). Such LESs are self-contained in a sense that once a shape function is assumed the remaining information is obtained from the ongoing LESs. In fact, we discuss later how also a shape function can be derived from LESs itself, making the entire procedure only minimally dependent on extraneous information input.

B. Comparison with the dynamic SGS modeling

At this point it is useful to note similarities and differences between the described procedure and the dynamic modeling approach since both employ the same Germano identity (45). The Germano identity does not invoke any specific SGS model but merely relates the SGS transfers computed for the full velocity field at two different cutoffs (here k_c and $(1/2)k_c$) to the SGS transfer at cutoff $(1/2)k_c$ computed for the resolved LES field. The dynamic modeling involves two steps. First, a SGS modeling expression must be selected; e.g., in the context of the present work it could be a wave-number-dependent eddy viscosity (50). It should be stressed, however, that the Germano identity does not impose restrictions on SGS models that may be considered. In addition to the Smagorinsky model the dynamic procedure has been applied to variety of other models, e.g., to the Bardina mixed model by Zang *et al.* [52] and to the Vreman model by You and Moin [53]. The second step in the dynamic approach is to determine model coefficients. While it was shown by Ghosal *et al.* [54] that it is possible to formulate a general integral equation for space- and time-dependent coefficients, in practice a limited number of coefficients is determined by the least squares method as originally proposed by Lilly [55]. In most cases just one coefficient is sought, in the current context C_m in (50), and the dynamic procedure, using (45), leads to

$$\int_0^{\frac{1}{2}k_c} C_m\left(\frac{1}{2}k_c\right) f_i\left(k|\frac{1}{2}k_c\right) 2k^2 E(k)\, dk - \int_0^{\frac{1}{2}k_c} C_m(k_c) f_i(k|k_c) 2k^2 E(k)\, dk = T_{\text{SGS}}^{\text{res}}\left(\frac{1}{2}k_c\right), \tag{52}$$

where the explicit notation is used to distinguish model application at different cutoffs. In principle this is one equation for two unknowns, $C_m(\frac{1}{2}k_c)$ and $C_m(k_c)$. Enforcing constant energy flux for the model at both cutoffs,

$$\int_0^{\frac{1}{2}k_c} C_m\left(\frac{1}{2}k_c\right) f_i\left(k|\frac{1}{2}k_c\right) 2k^2 E(k)\, dk = \int_0^{k_c} C_m(k_c) f_i(k|k_c) 2k^2 E(k)\, dk, \tag{53}$$

and the spectral form $k^{-5/3}$ for $E(k)$ produces a well-known inertial range scaling $C_m(k_c) = 2^{-4/3} C_m(\frac{1}{2}k_c)$, allowing us to compute the C_m coefficient for the cutoff k_c:

$$C_m(t) = \frac{T_{\text{SGS}}^{\text{res}}(\frac{1}{2}k_c)}{2^{4/3}\int_0^{\frac{1}{2}k_c} f_i(k|\frac{1}{2}k_c) 2k^2 E(k)\, dk - \int_0^{\frac{1}{2}k_c} f_i(k|k_c) 2k^2 E(k)\, dk}. \tag{54}$$

With the assumption (53) the above equation is equivalent to Eq. (51), and both can be rewritten in exactly the same form:

$$C_m(t) = \frac{T^{\rm res}_{\rm SGS}(\frac{1}{2}k_c)}{(1-b)\int_0^{k_c} f_i(k|k_c)2k^2E(k)\,dk}. \tag{55}$$

The difference between both methods is how the parameter b is determined. The dynamic procedure provides an explicit expression that depends on the model selected:

$$b = \frac{\int_0^{\frac{1}{2}k_c} f_i(k|k_c)2k^2E(k)\,dk}{\int_0^{k_c} f_i(k|k_c)2k^2E(k)\,dk}. \tag{56}$$

The present method determines b irrespective of the model, from a physical estimate of the global SGS transfer for a given velocity field. The difference arises because both approaches set different objectives. In the proposed approach the objective is to find the best estimate of the total SGS transfer using a resolved LES field. In the dynamic procedure the objective is to find the best estimate of model coefficients using a resolved LES field. The common feature is that both approaches use the Germano identity to accomplish their respective goals. In the dynamic procedure a model is selected first and the Germano identity is used subsequently to determine a model constant. In particular this implies that the predicted SGS transfer $T_{\rm SGS}(k_c)$ will depend not only on a given velocity field but also on a selected model; i.e., for the same velocity field but different models the dynamic procedure will give different values of $T_{\rm SGS}(k_c)$. The simplest example to illustrate such a behavior is to consider two eddy viscosity models, one that is nonzero for the entire resolved range $0 < k < k_c$ [e.g., (27)–(29)] and another one with a restricted spectral support $0.5k_c < k < k_c$ [e.g., (30)]. For the latter the integral in (45) vanishes, leading to $T_{\rm SGS}(k_c) = T^{\rm res}_{\rm SGS}(\frac{1}{2}k_c)$, or equivalently, the constant $b = 0$ in (55); for the other the formula (47) applies with the value of b determined independently of a model, where based on physical considerations $b = 0.4$ is chosen, which is also likely the maximum value consistent with energy transfer processes in the inertial range. Therefore, for a given velocity field the total SGS transfer predicted by the dynamic procedure, depending on the model, may vary between the total resolved SGS transfer $T^{\rm res}_{\rm SGS}$ and $(5/3)T^{\rm res}_{\rm SGS}$, the latter value corresponding to the eddy viscosity constant in k. In the proposed method the total SGS transfer as determined by the latter form is enforced for an arbitrary SGS model. On physical grounds the method that uses a unique value of the total SGS transfer for a unique velocity field is preferred to the method which predicts a range of model-dependent values. Nevertheless, the dynamic procedure is valuable and very successful in practice because the predicted range for total SGS transfer is in an approximate agreement with the expected range based on physical considerations. In particular, both methods will produce comparable values of b for classical models defined by shape functions f_0 and f_1.

V. RESULTS

A. Spherical, sharp spectral filter

For the purposes of testing the concepts we have performed multiple large eddy simulations. Because a large number of different models need to be evaluated, we have used a relatively low resolution of 32^3 mesh points in most cases. That resolution is consistent with other investigations that required multiple runs to test new SGS models (e.g., Langford and Moser [56]) and was found sufficient for drawing conclusions that were reinforced by performing several runs with the resolution increased to 64^3 modes. The majority of cases were initialized with the Kolmogoroff spectral form, $k^{-5/3}$, with no prefactors, and were run until a statistically steady state was reached. The simulations were continued in the steady state to collect statistics. Note that turbulence parameters defined at the end of Sec. II depend on the viscous dissipation ε, which is dominated by the high wave number part of the energy spectrum, not available in LESs. For high Reynolds numbers

TABLE I. Spectral models.

Case	Model
ivis	Eq. (28): $\frac{2}{3}C_K{}^{-3/2}$
iviscl	Eq. (27): $C_K{}^{-3/2}(0.441 + 15.2e^{-3.03k_c/k})$
ceddy	Eq. (50): $f_0 = 1$
CLeddy	Eq. (50): $f_1 = (0.441 + 15.2e^{-3.03k_c/k})$
CLedk4	Eq. (50): $f_2 = [D_2 + (k/k_c)^4]$
SVVmod	Eq. (50): $f_3 = \exp[-(\frac{1-k/k_c}{A-k/k_c})^2]$ for $k/k_c \leqslant A$; otherwise $f_3 = 0$

considered in this work the unknown viscous dissipation ε is assumed to be equal to the energy flux Π across the spectrum. In forced LESs we estimate $\Pi = \varepsilon$ in a steady state as a difference between the measured energy input rate by forcing and the known viscous dissipation in the resolved range. The viscous dissipation in the resolved range was found to be four orders of the magnitude less than estimated ε. Using this estimate the Taylor microscale Reynolds number Re_λ in all cases exceeded 10^4, confirming that considered LESs are for high Reynolds number turbulence where the Kolmogoroff theory should apply. The simulations were run for 2000 time steps, which corresponds to about seven large eddy turnover times T_e, and the results were generally averaged over the last three eddy turnover times. In order to facilitate distinguishing among different models in subsequent figures we will use notation summarized in Table I. In Table II we collect details of LESs for case "ivis" (eddy viscosity constant in k), which is representative of the models considered.

In Fig. 2 we plot results of LESs for two classical spectral eddy viscosity models given by expressions (27) and (28), with nondimensionalization given by (26). To emphasize the need for an appropriate SGS model in such simulations we also plot results for DNSs under the same conditions, the so called no-model LESs, and for the Bardina similarity model

$$\tau_{ij}^{\mathrm{sim}} = \overline{\bar{u}_i\,\bar{u}_j} - \bar{u}_i\,\bar{u}_j, \tag{57}$$

where the overbar signifies filtering with the Gaussian filter with the filter width $\Delta = 2\Delta x$. In both the latter cases a lack of a physically adequate SGS dissipation quickly leads to the energy equipartition for modes outside the forcing band, characterized by the energy spectrum proportional to k^2. On the other hand the models (27) and (28) tend to remain close to the spectral $k^{-5/3}$ shape throughout the simulation time. The dip in the spectra at the last wave number is caused by averaging over the wave number band centered at that wave number. Because of truncations performed as part

TABLE II. LES parameters.

Quantity	Value
Δt	0.005
N_{steps}	2000
ν	2.5×10^{-7}
u'^2	1.095
Forcing factor	1.00125
ε	0.519
λ	2.79×10^{-3}
Re_λ	1.17×10^4
L_p	1.35
T_e	1.29

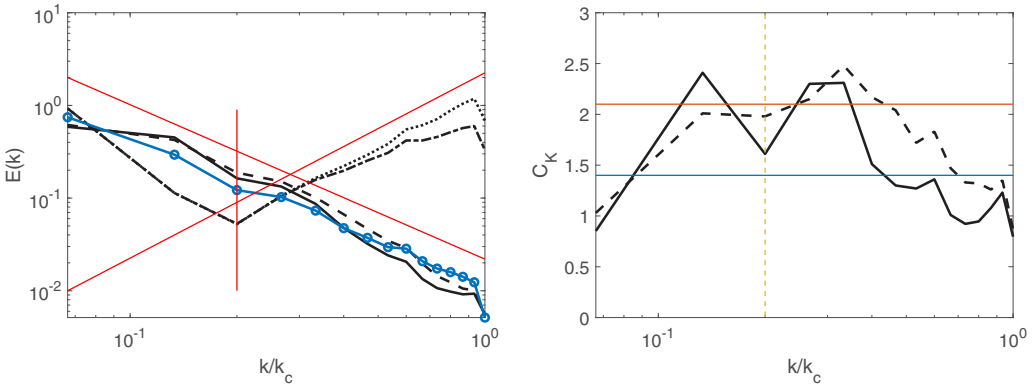

(a) Energy spectra (b) Compensated energy spectra

FIG. 2. Results for classical eddy viscosity models. Line with symbols ○: initial condition; solid line: case "ivis"; broken line: case "iviscl"; dotted line: no-model LESs; broken-dotted line: similarity model (57) with Gaussian filter. In this and all subsequent figures thin straight lines show, as appropriate, $-5/3$ and 2 slopes, and a boundary of the forcing band at $k = 3$. For compensated spectra (b) horizontal lines mark expected range of values for the Kolmogoroff constant.

of dealising, the modes in the band of finite thickness with wave numbers greater than the band center are set to zero, reducing the energy content in the last band compared with bands away from the cutoff.

The overall quality of predicted spectral slopes can be better evaluated by plotting compensated spectra in a form of a k-dependent Kolmogoroff function

$$C_K(k) = \frac{E(k)}{\varepsilon^{2/3} k^{-5/3}}. \tag{58}$$

According to experimental and DNS investigations, $C_K(k)$ is expected to be a constant with a value in the range 1.4–2.1 for the perfect Kolmogoroff range [57,58]. Function (58) is shown in Fig. 2(b) for both models at the end of respective runs. The values of $C_K(k)$ are not constant and fall only roughly within the expected range, and in both cases there are signs of overdissipation as the cutoff is approached. The Chollet-Lesieur model (27) provides a better prediction in a sense that $C_K(k)$ shows less variation than the prediction for the constant eddy viscosity model (28). We are not attempting to improve predictions by optimizing the model constant ${C_K}^{-3/2}$ but accept the recommendation of Chollet and Lesieur [22] $C_K = 1.4$. The results for these two classical models at the same, low resolution are consistent with results in the literature (see [22] and [23]) and can serve as benchmarks that any new modeling approach should meet or exceed.

The interscale energy transfer model has been implemented for three shape functions f_0, f_1, f_3, the first two corresponding to benchmark models with constant parameters. The energy spectra are shown in Fig. 3. It is seen that for functions f_0 and f_1 the spectra are in a good agreement with spectra obtained using benchmark models (Fig. 2). In fact, minor improvements are observed when compensated spectra shown in Fig. 3(b) are considered. However, for the function f_3 the energy spectrum does not match the $k^{-5/3}$ form: the spectral slope is flatter immediately after the forcing band and much steeper in the vicinity of the cutoff. The observed behavior is likely caused by an insufficient energy transfer from scales $k < (1/2)\, k_c$, where the eddy viscosity is zero, and an excessive transfer from scales $k > (1/2)\, k_c$, where the eddy viscosity is rapidly rising with k. We can thus conclude that the quality of LES predictions is dependent not just on properly capturing the total SGS transfer T_{SGS} but also on its proper distribution among resolved wave numbers $k < k_c$ by a model shape function.

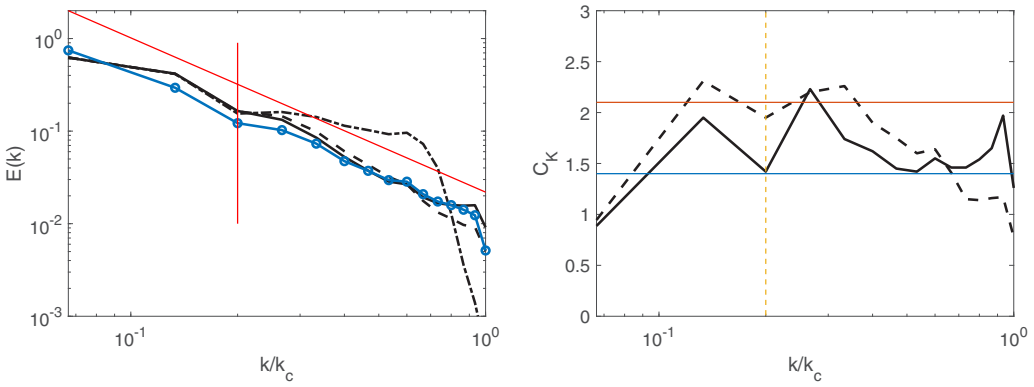

(a) Energy spectra (b) Compensated energy spectra

FIG. 3. Models with shape functions f_0, f_1, and f_3. Line with symbols ○: initial condition; solid line: case "ceddy"; broken line: case "CLeddy"; broken-dotted line: case "SVVmod."

To assess the sensitivity of LES predictions to changes in the SGS transfer scale distribution we have used the model (29) for function f_2 with four different values of parameter $D_2 = 1.10,\ 0.55,\ 0.275,\ 0$. The ratio of the plateau value of the eddy viscosity to the peak value at the cusp decreases from about 0.5 for $D_2 = 1.10$ to zero, with intermediate values of 0.35 and 0.22 for $D_2 = 0.55$ and $D_2 = 0.275$, respectively. The value $D_2 = 0.55$ corresponds to the theoretical distribution (27), while values $D_2 = 1.10$ and $D_2 = 0.275$ give respectively larger and smaller relative weight to the plateau contribution to the total transfer. The value of $D_2 = 0$ concentrates the SGS transfer in scales closer to the cutoff, similarly to the SSV case (30). The energy spectra for all cases are shown in Fig. 4. It is seen that the case $D_2 = 0$ produces similar behavior as the SSV viscosity, while the remaining three cases, $D_2 > 0$, show acceptable agreement with the $k^{-5/3}$ spectrum. However, as the constant D_2 decreases the spectra begin to deteriorate, which is better seen in the plot of the compensated spectra shown in Fig. 4(b).

Additional insight into the dependence of spectral results on a shape function can be gained by investigating a wave number distribution of the resolved SGS energy transfer $T^{\rm res}_{\rm SGS}(\mathbf{k}|ak_c)$ [see Eq. (39)]. This quantity, computed for $a = 1/2$, and cast in the form of the k-dependent eddy viscosity (25), is shown in Fig. 5 for LES cases with $D_2 = 1.10,\ 0.55,\ 0.275$, and for the LES case run

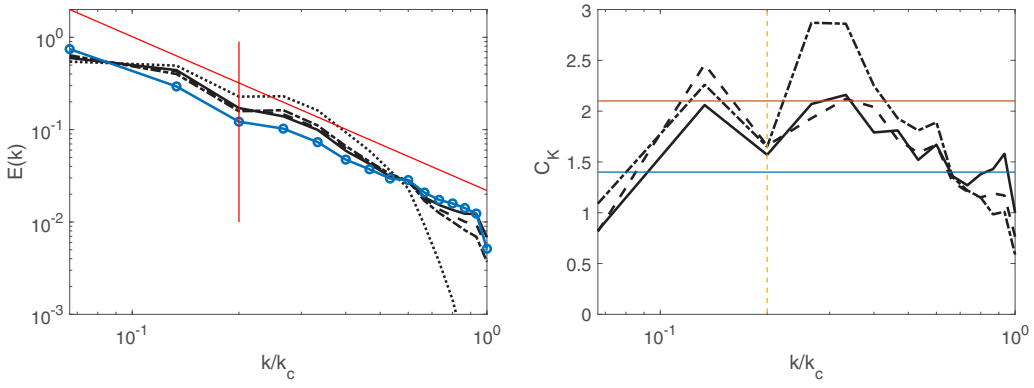

(a) Energy spectra (b) Compensated energy spectra

FIG. 4. Model with shape function f_2 (case "CLedk4") and different values of D_2. Line with symbols ○: initial condition; solid line: $D_2 = 1.10$; broken line: $D_2 = 0.55$; broken dotted line: $D_2 = 0.275$; dotted line: $D_2 = 0$.

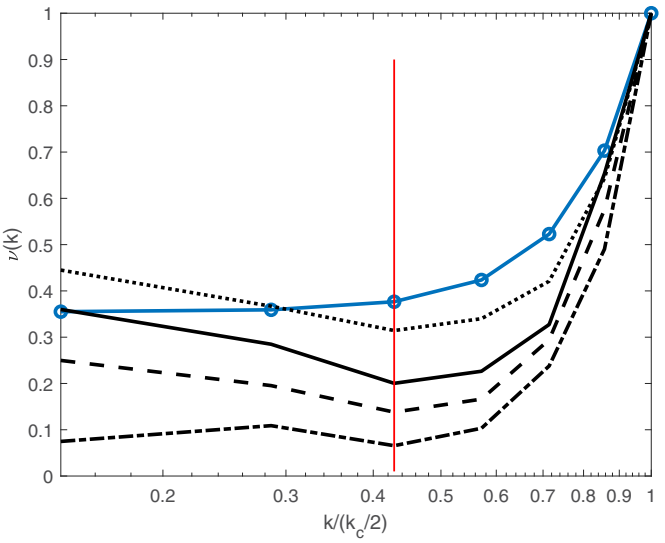

FIG. 5. Spectral eddy viscosities computed from LESs performed with shape function f_2 (case "CLedk4") and different values of D_2. Solid line: $D_2 = 1.10$; broken line: $D_2 = 0.55$; broken dotted line: $D_2 = 0.275$. Dotted line: eddy viscosity from LES data for case "ceddy"; line with symbols ○: analytical expression (29).

with the eddy viscosity constant in k (function f_0; see Fig. 3). All four curves are normalized with their peak values at $k/k_c = 1$ and compared with the theoretical shape function f_2 for $D_2 = 0.55$. The curves obtained from LES data exhibit qualitatively the same behavior as the theoretical eddy viscosity: a plateau for $k/k_c \leqslant 1/2$ followed by a cusp as the cutoff wave number is approached. Also, a plateau level obtained from LES data is correlated with the plateau level of a shape function used in LESs, i.e., as D_2 in LESs decreases so does the computed plateau level. Quantitatively, however, the plateau values computed from LES data can be by a factor of 2 less than plateau values for shape functions used to generate those data. The most likely explanation for this quantitative inconsistency is that in computing $T^{\rm res}_{\rm SGS}(\mathbf{k}|(1/2)k_c)$ nonlinear interactions with unresolved scales $k > k_c$ are unaccounted for, reducing the SGS energy transfer from the range $k < (1/2)\, k_c$, and thus the level of the eddy viscosity in that range. Nevertheless, these results are encouraging, showing that the assumed shape functions are in many respects consistent with the corresponding quantities computed from actual LES data. This also suggests that rather than prescribing and testing various shape functions it should be possible to infer a shape function directly from LESs, further reducing dependence of the method on information extraneous to actual simulations. A simple strategy is to start LESs with the eddy viscosity constant in k (shape function f_0) and, after nonlinear energy transfer is established, compute a shape function from the analysis of $T^{\rm res}_{\rm SGS}(\mathbf{k}|(1/2)k_c)$. As suggested by Fig. 5 such a function will constitute a very good fit to the theoretical shape function for a given LES and can be used to continue the simulation. We have tested the viability of such an approach by performing a precursor LES run with the shape function f_0 for about half of the eddy turnover time, extracting a numerical shape function from the LES data at the end of the precursor run, and continuing LESs with the numerical shape function for the same time as all other analyzed simulations. In Fig. 6 we compare results from this procedure with results of continuing the run with the model f_0 for the same time period. Both runs produce spectra of comparable quality though with different values of the Kolmogoroff constant outside the forcing band.

B. Additional topics: Different resolutions, different initial conditions, and graded filters

To assess the dependence of the method on numerical resolution for several cases LESs have been performed with 64^3 modes and compared with results obtained in simulations with 32^3 modes

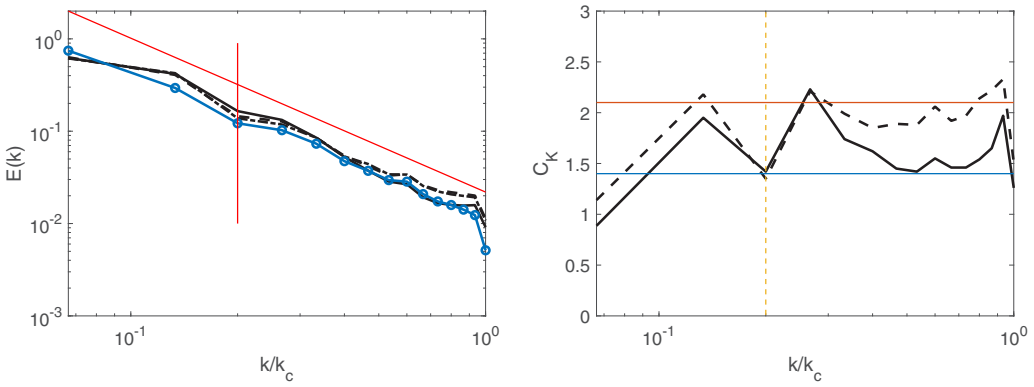

(a) Energy spectra (b) Compensated energy spectra

FIG. 6. A model with a shape function computed from a precursor LES. Line with symbols ○: initial condition; solid line: case "ceddy"; broken line: results using a shape function computed from case "ceddy."

reported in the previous section. In Fig. 7 we show such a comparison for the case "ceddy" (see Table I). Both runs were initialized with the inertial range spectral form and the same seed for a random number generator and were run for the same number of time steps $N_{\text{steps}} = 2000$ with the same time step $\Delta t = 2.5 \times 10^{-7}$. The spectrum for the lower resolution case is shifted to the right of the spectrum for the higher resolution case because wave numbers k in both cases are normalized by the cutoff wave number k_c. The extent of the forcing band for each case is indicated by short vertical lines, and a straight diagonal has a slope of $-5/3$. The raw spectra for both cases are not smooth, especially inside the forcing bands, because of small number of modes captured by the averaging procedure over shells with thickness $\Delta k = 1$. The choppiness of spectra diminishes for the higher resolution case, especially for larger k/k_c, and the fluctuations can be further decreased by considering thicker shells with $\Delta k = 2$. However, the important observation is that outside forcing

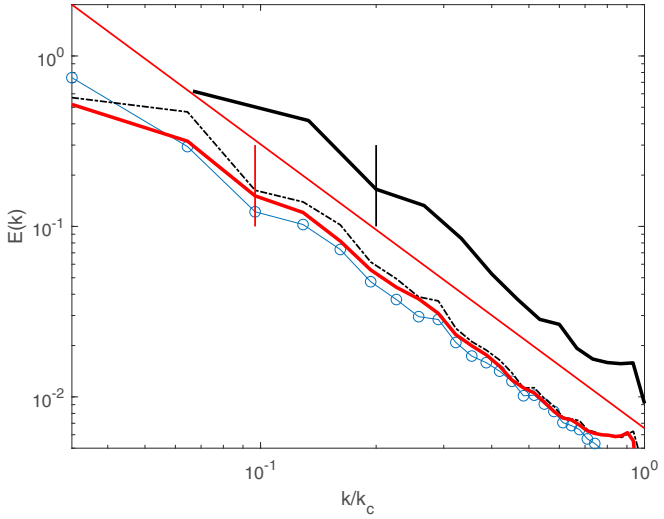

FIG. 7. Energy spectra for the model "ceddy" at different resolutions. Straight diagonal line: $\sim k^{-5/3}$. Line with symbols ○: initial condition; solid line above $k^{-5/3}$ line: resolution 32^3 modes; broken-dotted line: resolution 64^3 modes; solid line below $k^{-5/3}$ line: resolution 64^3 with averaging over thicker shells.

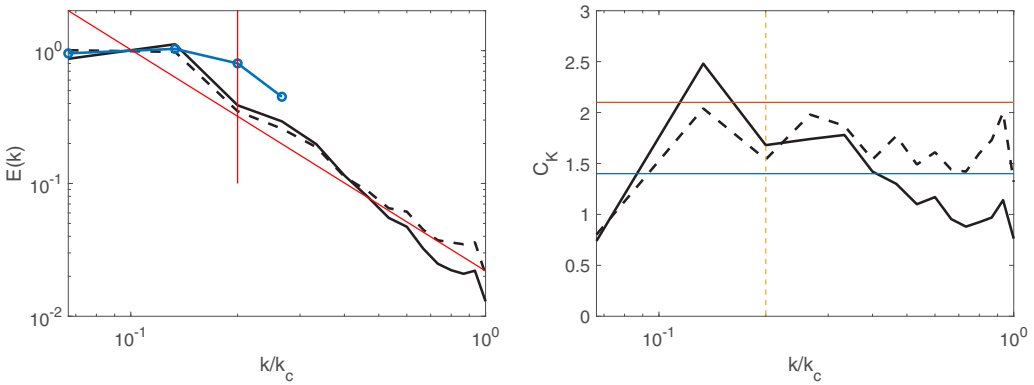

(a) Energy spectra (b) Compensated energy spectra

FIG. 8. A pulse spectrum initial condition. Line with symbols ○: initial condition; solid line: case "ivis"; broken line: case "ceddy."

bands both spectra follow each other closely and are in a good agreement with the Kolmogoroff form. We conclude that while higher resolution results are smoother, there are no indications that the dynamics predicted by the method is dependent on the two resolutions considered.

Forced turbulence spectra tend asymptotically toward the Kolmogoroff $k^{-5/3}$ form, and SGS models should be able to capture this behavior independently of the initial condition. We have performed several LESs with a pulse-type initial condition where $E(k) = 0$ for $k > 4$. In Fig. 8 we show the initial spectrum and results of its evolution in LESs obtained using the k-independent theoretical eddy viscosity (28) and the corresponding interscale transfer model with the constant function $f_0 = 1$. Both models lead to spectra qualitatively consistent with expected behavior though the theoretical eddy viscosity is somewhat overdissipative. Note that the overall energy level for spectra in these runs is more than twice larger than in LESs initialized with the $k^{-5/3}$ function because the forcing algorithm leads to larger energy input for the flatter initial spectrum. The fact that the final spectra in all LESs are consistent with the $k^{-5/3}$ form with a reasonable value of the Kolmogoroff constant is encouraging, indicating that the proposed modeling approach properly captures dynamics of turbulence at high Reynolds numbers.

While a sharp spectral filter is a natural choice in LESs and turbulence studies using Fourier modes, in LESs performed with finite volume or finite difference numerical codes graded filters are normally employed. Additionally, for Cartesian grids 3D filters are written as a product of 1D filters. It is thus natural to ask if and how the modeling procedure proposed here can be extended to such a more typical LES framework in the physical space representation. To investigate this question we have used Gaussian and box filters, both with the filter width $\Delta = 2\Delta x$. Specifically, the 1D Gaussian filter kernel is

$$G(x, x') = \sqrt{\frac{6}{\pi \Delta^2}} \exp\left(-\frac{6|x - x'|^2}{\Delta^2}\right) \tag{59}$$

and the 1D box filter kernel

$$G(x, x') = \begin{cases} 1/\Delta & \text{if } |x - x'| \leqslant \Delta/2, \\ 0 & \text{otherwise.} \end{cases} \tag{60}$$

The filtering operation in Cartesian coordinates for an arbitrary function $f(x, y, z)$ is then given by the formula

$$\overline{f}(x, y, z) = \int dx'\, dy'\, dz' G(x, x') G(y, y') G(z, z') f(x', y', z'). \tag{61}$$

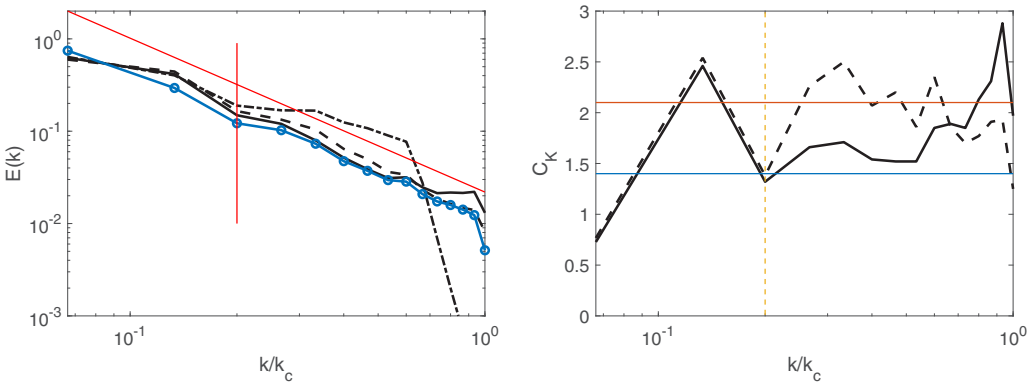

(a) Energy spectra (b) Compensated energy spectra

FIG. 9. Models with shape functions f_0, f_2, and f_3 using Gaussian filtering. Line with symbols ○: initial condition; solid line: case "ceddy"; broken line: case "CLedk4"; broken-dotted line: case "SVVmod."

We have performed LESs using the proposed procedure in exactly same form as described in previous sections, merely replacing the sharp spectral filtering by graded filters as given by formulas above. There is a subtle difference in interpretation of quantities computed using the sharp spectral filter and graded physical space filters. For both cases all quantities in LESs are represented on a mesh with a finite mesh size Δx, implying spectral support with a cutoff wave number $k_c = \pi/\Delta x$. When a sharp spectral filter is applied at an intermediate wave number, say $(1/2)k_c$, the resulting filtered quantities lose completely information about scales $(1/2)k_c < k < k_c$; those scales are truly unknown, subgrid scales. In case of the physical space filters a filtered field still has the same spectral support as the full, unfiltered field, and, for invertible filters, there is no information loss. In such a case the velocity field $u_i' = u_i - \overline{u}_i$ is often called a subfilter velocity. A good discussion of how differences between sharp spectral filter and graded physical space filters affect interpretation of LES results is given by Langford and Moser [47] and Domaradzki and Adams [59]). While these differences could suggest that physical quantities computed with different filters in our modeling procedure could lead to incongruent outcomes, we were surprised to find that this was not the case. This conclusion is confirmed by plots of energy spectra shown in Fig. 9 obtained in LESs using the Gaussian filter and shape functions f_0, f_2, and f_3. Very similar results were obtained using the box filter, so they are not shown here. The results are in a close agreement with the corresponding results of LESs performed with the spectral filter, shown in Fig. 3. Note that since shape functions f_0 and f_2 have a direct physical space representation, these two models can be implemented entirely in the physical space if filters (59) or (60) are used. In that case $T_{\rm SGS}^{\rm res}(\frac{1}{2}k_c)$ required in the model is obtained using the physical space formula (21) for $\epsilon_{\rm SGS}(\mathbf{x})$.

VI. CONCLUSIONS

A subgrid-scale (SGS) modeling procedure has been developed that is based on the interscale energy transfer among resolved scales in an actual LESs. The total, unknown SGS transfer is estimated using the computed SGS transfer within the resolved range and a few, well-established facts concerning turbulence dynamics at very high Reynolds numbers. The total SGS transfer then becomes a first-order constraint that any proposed SGS eddy viscosity model should satisfy. The procedure was evaluated using low-resolution LESs for forced, high Reynolds number isotropic turbulence for which the inertial range dynamics is expected. Several common models, characterized by different shape functions for a distribution of SGS transfer among scales of motion, were implemented and tested. It was concluded that details of shape functions can be considered as a less important, second-order constraint, in a sense that an entire class of shape functions would lead to

very similar spectral results in LESs. In particular, shape functions for wave-number-dependent eddy viscosity, suggested by the classical theories of turbulence, with a low wave number plateau and a cusp at the cutoff wave number were able to produce energy spectra in as good agreement with the inertial range form as LES results reported in the literature for models with fixed, time-independent coefficients. On the other hand models using shape functions with a cusp but without a low wave number plateau were unable to produce or maintain the inertial range spectrum in LESs. Therefore, in addition to satisfying quantitatively the global SGS energy transfer constraint, a qualitatively correct wave number distribution of the SGS transfer is needed to produce good LES results. It should be noted that the eddy viscosity computed from DNS results at low Reynolds numbers is characterized by a cusp and a negligible value of the plateau [43], similar to the SSV model and the shape function f_2 with $D_2 = 0$. This strongly suggests that as the Reynolds number of a flow decreases, the plateau value decreases as well, eventually going to zero as the dynamics become dominated by viscous effects and energy spectra become much steeper than the Kolmogoroff form. In the present modeling procedure such a behavior could be accounted for by making constant D_2 dependent on Reynolds number. However, it was shown that prescribing the SGS transfer distribution through shape functions may be replaced entirely by deriving shape functions from the data available in a given LES. This has a potential of making LES fully self-contained, with required information about the total SGS transfer and its scale distribution available from an LES run in question.

We have also briefly addressed a question how to extend the proposed modeling procedure to a framework of the physical space representation, typical of SGS modeling for practical applications. We have determined that it is possible to compute the total SGS energy transfer constraint using the physical space formula (23) and physical space filters, implemented as a tensor product of 1D filters (59) and (60) in Cartesian coordinates. We have also proposed a general expression f_2 for a shape function that has a straightforward physical space representation; it additionally allows us to control the plateau level of a spectral eddy viscosity through a free parameter D_2.

Finally, one may also speculate how the proposed method could be used for LESs of inhomogenous flows, which must be simulated in the physical representation. One obvious approach would be to use the total estimated SGS transfer as a constraint on a model constant, in the same way as the dynamic procedure uses the Germano identity. Another one could be using the total SGS transfer as an additional constraint in the classical dynamic procedure, i.e., optimizing model coefficients with respect to the Germano identity and the total SGS transfer.

ACKNOWLEDGMENT

The author is grateful to Prof. P. K. Yeung for making his excellent numerical code available for research in isotropic turbulence.

[1] A. Leonard, Energy cascade in large eddy simulations of turbulent fluid flows, Adv. Geophys. A **18**, 237 (1974).

[2] S. Ghosal and P. Moin, The basic equations for the large eddy simulation of turbulent flows in complex geometry, J. Comp. Phys. **118**, 24 (1995).

[3] O. V. Vasilyev, T. S. Lund, and P. Moin, A general class of commutative filters for LES in complex geometries, J. Comput. Phys. **146**, 82 (1998).

[4] B. Galperin and e. S. A. Orszag, *Large Eddy Simulation of Complex Engineering and Geophysical Flows* (Cambridge University Press, Cambridge, 1993).

[5] M. Lesieur and O. Metais, New trends in large-eddy simulations of turbulence, Annu. Rev. Fluid Mech. **28**, 45 (1996).

[6] U. Piomelli, Large-eddy simulations: Achievements and challenges, Prog. Aero. Sci. **35**, 335 (1999).

[7] C. Meneveau and J. Katz, Scale-invariance and turbulence models for large eddy simulations, Annu. Rev. Fluid Mech. **32**, 1 (2000).
[8] S. Pope, *Turbulent Flows* (Cambridge University Press, Cambridge, 2000).
[9] P. Sagaut, *Large-Eddy Simulation for Incompressible Flows*, 2nd ed. (Springer-Verlag, Berlin, 2002).
[10] J. Smagorinsky, General circulation experiments with the primitive equations, Mon. Weath. Rev. **93**, 99 (1963).
[11] M. Germano, U. Piomelli, P. Moin, and W. Cabot, A dynamic subgrid-scale eddy viscosity model, Phys. Fluids **3**, 1760 (1991).
[12] J. P. Boris, F. F. Grinstein, E. S. Oran, and R. L. Kolbe, New insights into large eddy simulation, Fluid Dyn. Res. **10**, 199 (1992).
[13] L. G. Margolin and W. J. Rider, A rationale for implicit turbulence modeling, Int. J. Numer. Meth. Fluids **39**, 821 (2002).
[14] F. Grinstein and C. Fureby, Recent progress on MILES for high Reynolds number flows, J. Fluids Eng. **124**, 848 (2002).
[15] *Implicit Large Eddy Simulation: Computing Turbulent Fluid Dynamics*, edited by F. F. Grinstein, L. G. Margolin, and W. J. Rider (Cambridge University Press, Cambridge, 2007).
[16] D. Lilly, The representation of small-scale turbulence in numerical simulation experiments, in *Proc. IBM Scientific Computing Symp. on Environmental Sciences*, edited by H. H. Goldstine (IBM, Yorktown Heights, NY, 1967) pp. 195–210.
[17] T. Eidson, Numerical simulation of the turbulent Rayleigh-Bénard problem using subgrid modelling, J. Fluid Mech. **158**, 245 (1985).
[18] U. Piomelli, High Reynolds number calculations using the dynamic subgrid-scale stress model, Phys. Fluids A **5**, 1484 (1993).
[19] S. Toosi and J. Larsson, Anisotropic grid-adaptation in large eddy simulations, Comput. Fluids **156**, 146 (2017).
[20] R. Kraichnan, Eddy viscosity in two and three dimensions, J. Atmos. Sci. **33**, 1521 (1976).
[21] D. Leslie and G. Quarini, The application of turbulence theory to the formulation of subgrid modelling procedures, J. Fluid Mech. **91**, 65 (1979).
[22] J. Chollet and M. Lesieur, Parameterization of small scales of three-dimensional isotropic turbulence utilizing spectral closures, J. Atmos. Sci. **38**, 2767 (1981).
[23] M. Lesieur, *Turbulence in Fluids*, 3rd ed. (Kluwer Academic, Dordrecht, 1997).
[24] M. Lesieur, O. Metais, and P. Comte, *Large Eddy Simulations of Turbulence* (Cambridge University Press, Cambridge, 2005).
[25] O. Metais and M. Lesieur, Spectral large-eddy simulations of isotropic and stably-stratified turbulence, J. Fluid Mech. **239**, 157 (1992).
[26] J. Domaradzki and R. Rogallo, Local energy transfer and nonlocal interactions in homogeneous, isotropic turbulence, Phys. Fluids A **2**, 413 (1990).
[27] J. Domaradzki, W. Liu, C. Härtel, and L. Kleiser, Energy transfer in numerically simulated wall-bounded turbulent flows, Phys. Fluids **6**, 1583 (1994).
[28] J. A. Domaradzki and W. Liu, Approximation of subgrid-scale energy transfer based on the dynamics of resolved scales of turbulence, Phys. Fluids **7**, 2025 (1995).
[29] J. Domaradzki, Analysis of energy transfer in direct numerical simulations of isotropic turbulence, Phys. Fluids **31**, 2747 (1988).
[30] P. Yeung and J. Brasseur, The response of isotropic turbulence to isotropic and anisotropic forcing at the large scales, Phys. Fluids A **3**, 413 (1991).
[31] J. Domaradzki, W. Liu, and M. Brachet, An analysis of subgrid-scale interactions in numerically simulated turbulence, Phys. Fluids A **5**, 1747 (1993).
[32] R. M. Kerr, J. A. Domaradzki, and G. Barbier, Small-scale properties of nonlinear interactions and subgrid-scale energy transfer in isotropic turbulence, Phys. Fluids **8**, 197 (1996).
[33] J. A. Domaradzki and D. Carati, An analysis of the energy transfer and the locality of nonlinear interactions in turbulence, Phys. Fluids **19**, 085112 (2007).

[34] M. Lee and R. D. Moser, Spectral analysis of the budget equation in turbulent channel flows at high Reynolds number, J. Fluid Mech. **860**, 886 (2019).
[35] A. Cimarelli, E. De Angelis, and C. M. Casciola, Paths of energy in turbulent channel flows, J. Fluid Mech. **715**, 436 (2013).
[36] A. Cimarelli, E. De Angelis, J. Jiménez, and C. M. Casciola, Cascades and wall-normal fluxes in turbulent channel flows, J. Fluid Mech. **796**, 417 (2016).
[37] B. W. Anderson and J. A. Domaradzki, A subgrid-scale model for large-eddy simulation based on the physics of interscale energy transfer in turbulence, Phys. Fluids **24**, 065104 (2012).
[38] M. Anderer, Explicit subgrid-scale models for the simulation of turbulent flows with high order discontinuous Galerkin methods, Technical report, University of Stuttgart, 2015.
[39] J. Bardina, J. Ferziger, and W. Reynolds, Improved turbulence models based on large eddy simulation of homogeneous incompressible turbulence, Technical Report TF-19, Stanford University, 1983.
[40] R. Rogallo, Technical Report Technical Memorandum No. 81315, National Aeronautics and Space Administration Technical Memorandum (1981).
[41] P. Yeung and S. Pope, An algorithm for tracking fluid particles in numerical simulations of homogeneous turbulence, J. Comput. Phys. **79**, 373 (1988).
[42] N. P. Sullivan, S. Mahalingam, and R. M. Kerr, Deterministic forcing of homogeneous, isotropic turbulence, Phys. Fluids **6**, 1612 (1994).
[43] J. A. Domaradzki, R. Metcalfe, R. Rogallo, and J. Riley, Analysis of Subgrid-Scale Eddy Viscosity with Use of Results from Direct Numerical Simulations, Phys. Rev. Lett. **58**, 547 (1987).
[44] J. Chollet, Two-point closures as a subgrid-scale modeling tool for large eddy simulations, in *Turbulent Shear Flows IV*, edited by L. J. S. Bradbury, F. Durst, B. E. Launder, F. W. Schmidt, and J. H. Whitelaw (Springer-Verlag, Berlin Heidelberg, 1985).
[45] G.-S. Karamanos and G. E. Karniadakis, A spectral vanishing viscosity method for large-eddy simulations, J. Comput. Phys. **163**, 22 (2000).
[46] E. Lamballais, V. Fortuné, and S. Laizet, Straightforward high-order numerical dissipation via the viscous term for direct and large eddy simulation, J. Comp. Phys. **230**, 3270 (2011).
[47] J. A. Langford and R. D. Moser, Optimal LES formulations for isotropic turbulence, J. Fluid Mech. **398**, 321 (1999).
[48] R. Kraichnan, The structure of isotropic turbulence at very high Reynolds numbers, J. Fluid Mech. **5**, 497 (1959).
[49] R. Kraichnan, Inertial-range transfer in two- and three-dimensional turbulence, J. Fluid Mech. **47**, 525 (1971).
[50] J. Domaradzki and D. Carati, A comparison of spectral sharp and smooth filters in analysis of nonlinear interactions and energy transfer in turbulence, Phys. Fluids **19**, 085111 (2007).
[51] N. Park and k. Mahesh, A velocity-estimation subgrid model constrained by subgrid scale dissipation, J. Comp. Phys. **227**, 4190 (2008).
[52] Y. Zang, R. Street, and J. Koseff, A dynamic mixed subgrid-scale model and its applications to turbulent recirculating flows, Phys. Fluids **5**, 318 (1993).
[53] D. You and P. Moin, A dynamic global-coefficient subgrid-scale eddy-viscosity model for large-eddy simulation in complex geometries, Phys. Fluids **19**, 065110 (2007).
[54] S. Ghosal, T. Lund, P. Moin, and K. Akselvoll, A dynamic localization model for large-eddy simulation of turbulent flows, J. Fluid Mech. **286**, 229 (1995).
[55] D. Lilly, A proposed modification of the Germano subgrid-scale closure method, Phys. Fluids **4**, 633 (1992).
[56] J. A. Langford and R. D. Moser, Optimal large-eddy simulation results for isotropic turbulence, J. Fluid Mech. **521**, 273 (2004).
[57] K. R. Sreenivasan, On the universality of the Kolmogorov constant, Phys. Fluids **7**, 2778 (1995).
[58] R. Kerr, Velocity, scalar and transfer spectra in numerical turbulence, J. Fluid Mech. **211**, 309 (1990).
[59] J. A. Domaradzki and N. A. Adams, Direct modelling of subgrid scales of turbulence in large eddy simulations, J. Turbulence **3**, N24 (2002).